International Journal of Electrical and Power Engineering 6 (2): 66-76, 2012
ISSN: 1990-7958

Performance Characteristics of the Switched Reluctance Motor in Electric Vehicle During Acceleration at Variable Turn on and Turn off Angle

[2]Fathy El Said Abdel-Kader, [1]M.Z. Elsherif, [1]Nasser M.B. Abdel-Rehim and [1]Mohamed M. Fathy
[1]Faculty of Engineering, Benha University, 108 Shoubra St., Cairo, Egypt
[2]Faculty of Engineering, Menofia University, G.A. Nasser St., Shibin El Kom, Egypt

Abstract: In this study, the equations describing the performance of the electric vehicle are derived. Performance characteristics for each part in the vehicle system are obtained when the vehicle is accelerated under variable turn on and turn off angles while the terminal voltage is held constant.

Key words: Switched reluctance motor, SRM, electric vehicle, acceleration mode, Egypt

INTRODUCTION

The Internal Combustion Engine (ICE) vehicle at the present is a major source of urban pollution. According to figures released by the US Environmental Protection Agency (EPA), conventional ICE vehicles currently contribute 40-50% of ozone (Nonmethane Organic Gases, NMOG), 80-90% of carbon monoxide (CO) and 50-60% of air toxins (Nitrogen Oxides, NOx) found in urban areas. Beside air pollution, the other main objection regarding ICE automobiles is their extremely low efficiency use of fossil fuel.

Hence, the problem associated with ICE automobiles is threefold: environmental, economical as well as political. These concerns have forced governments all over the world to consider alternative vehicle concepts (Ehsani *et al*., 1997, 2005; Husain, 2005). Electric Vehicles (EV) offer the most promising solutions to reduce vehicular emissions.

EV constitute the only commonly known group of automobiles that qualified as Zero Emission Vehicles (ZEVs). These vehicles use electric motors for propulsion and batteries as electrical energy storage devices (Ehsani *et al*., 1997; Husain, 2005). Figure 1 shows the drivetrain of the electric vehicle.

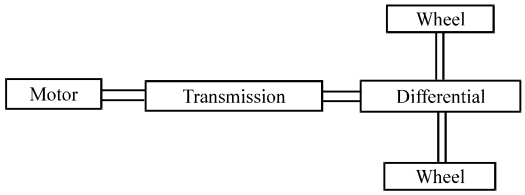

Fig. 1: The EV drivetrain

Switched Reluctance Motor (SRM) are perhaps the simplest of electrical machines. They consist of a stator with excitation windings and a magnetic rotor with saliency. Rotor conductors are not required because torque is produced by the tendency of the rotor to align with the stator produced flux wave in such a fashion as to maximize the stator flux linkages that result from a given applied stator current.

Due to simple and rugged motor construction, low weight, potentially low production cost, undemanding cooling, excellent torque-speed characteristics, high torque density, high operating efficiency and inherent fault tolerance, Switched Reluctance Motor (SRM) drives are emerging as an attractive solution for Electric Vehicle (EV) applications (Husain and Islam, 1999; Rahman *et al*., 2000; Sadeghi *et al*., 2007). Traction performances of EVs depend on the performances of SRM drives. Hence, the excellent motoring operation of SRMs is important for EVs with high performances.

MATERIALS AND METHODS

Performance equations of the EV with acceleration mode: To investigate the EV performance at acceleration it will be assumed that the vehicle is accelerated with the motor drive is fed from a constant DC voltage source with a variable turn on and turn off angle. The voltage equation of each phase winding can be expressed as:

$$v = iR + \frac{d\lambda(i,\theta)}{dt} \quad (1)$$

Neglecting the saturation of the magnetic circuit, the phase flux linkage can be expressed by:

Corresponding Author: Fathy El Said Abdel-Kader, Faculty of Engineering, Menofia University, G.A. Nasser St., Shibin El Kom, Egypt

$$\lambda(i,\theta) = L(\theta)i \tag{2}$$

By substitution from Eq. 2 into 1, the motor phase voltage can be written as:

$$v = iR + L(\theta)\frac{di}{dt} + i\frac{dL(\theta)}{dt} \tag{3}$$

Also, Eq. 3 can be rewritten as:

$$v = iR + L(\theta)\frac{di}{d\theta}\frac{d\theta}{dt} + i\frac{dL(\theta)}{d\theta}\frac{d\theta}{dt} \tag{4}$$

At steady state, the motor speed can be determined as a function of the rotor position by:

$$\omega = \frac{d\theta}{dt} \tag{5}$$

Where:
ω = The motor speed in elec. rad sec^{-1}
θ = The rotor position in elec. rad

Substituting from Eq. 5 into 4, the motor phase voltage can be expressed as:

$$v = iR + L(\theta)\omega\frac{di}{d\theta} + i\omega\frac{dL(\theta)}{d\theta} \tag{6}$$

Where the three terms of Eq. 6 represents the resistive drop, the self and rotational EMF, respectively. Finally after rearranging Eq. 6, the motor phase voltage can be rewritten as:

$$v = \left(R + \omega\frac{dL(\theta)}{d\theta}\right)i + \omega L(\theta)\frac{di}{d\theta} \tag{7}$$

From Fig. 2, the motor phase inductance can be represented as a function of the rotor position as:

$$\begin{aligned} L(\theta) &= L_u && 0 \le \theta \le \theta_i \\ L(\theta) &= k_1\theta - k_2 && \theta_i \le \theta \le \pi \\ L(\theta) &= -k_1\theta - k_3 && \pi \le \theta \le (2\pi - \theta_i) \\ L(\theta) &= L_u && (2\pi - \theta_i) \le \theta \le 2\pi \end{aligned} \tag{8}$$

The constants k_1-k_3 and θ_i are equal:

$$k_1 = \frac{L_a - L_u}{\pi - \theta_i};\quad k_2 = \frac{L_a\theta_i - L_u\pi}{\pi - \theta_i}$$

$$k_3 = \frac{-\pi(L_a - L_u) - L_a(\pi - \theta_i)}{\pi - \theta_i}$$

$$\theta_i = \pi - N_r\beta_r$$

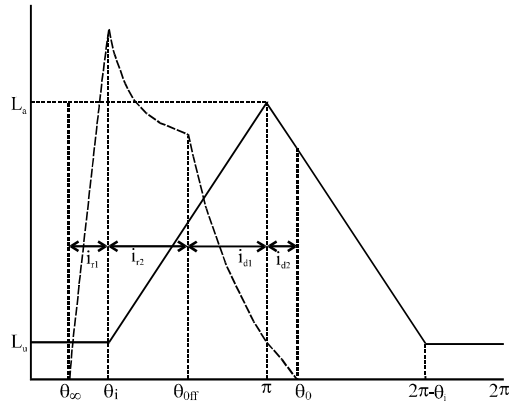

Fig. 2: Motor phase inductance and current against the rotor position

According to the motor phase voltage, there are two modes of operation of the SRM. At the first mode of operation, the motor phase voltage is connected to the DC supply Voltage (Vs), thus the motor phase current will be increases. At the second mode, the applied voltage on the motor phase is the negative value of the DC supply voltage, thus the motor phase current will be decays to zero value.

Substituting from Eq. 8 into 7 taking into account the specified modes of operation, the motor phase current can be obtained for each rotor position range included in Fig. 2 as:

$$\begin{aligned} i_{r1}(\theta) &= \frac{V_s}{R}\left(1 - e^{-(\theta-\theta_{on})R/(\omega L_u)}\right);\quad \theta_{on} \le \theta \le \theta_i \\ i_{r2}(\theta) &= \frac{V_s}{R + k_1\omega} + \left(i_{r1}(\theta_i) - \frac{V_s}{R + k_1\omega}\right) \\ &\quad \left(\frac{k_1\theta_i - k_2}{k_1\theta - k_2}\right)^{\left(\frac{R+k_1\omega}{k_1\omega}\right)};\quad \theta_i \le \theta \le \theta_{off} \\ i_{d1}(\theta) &= \frac{-V_s}{R + k_1\omega} + \left(i_{r2}(\theta_{off}) + \frac{V_s}{R + k_1\omega}\right) \\ &\quad \left(\frac{k_1\theta_{off} - k_2}{k_1\theta - k_2}\right)^{\left(\frac{R+k_1\omega}{k_1\omega}\right)};\quad \theta_{off} \le \theta \le \pi \\ i_{d2}(\theta) &= \frac{-V_s}{R - k_1\omega} + \left(i_{d1}(\pi) + \frac{V_s}{R - k_1\omega}\right) \\ &\quad \left(\frac{-k_1\pi - k_3}{-k_1\theta - k_3}\right)^{\left(\frac{R-k_1\omega}{-k_1\omega}\right)};\quad \pi \le \theta \le \theta_0 \end{aligned} \tag{9}$$

Where these equations are derived to represent the following range for the turn on and turn off angle: $\theta_{on} < \theta_i$ and $\theta_{off} < \pi$. Also θ_0 is the angle at which the motor phase current equal zero after decaying. This angle can be determined from Eq. 9 by putting ($i_{d2} = 0$ and $\theta = \theta_0$):

$$\theta_0 = \frac{1}{L_a - L_u}\left(\frac{-L_a(\pi-\theta_i)(R-k_1\omega)i_{d1}(\pi)+V_s^{k_4}}{V_s^{k_4}} + \pi(L_a-L_u)+L_a(\pi-\theta_i)\right) \quad (10)$$

Where the constant k_4 is equal $k_4 = -k_1\omega/R - k_{1\omega}$. Therefore, the motor torque is expressed by:

$$T_e = \frac{1}{2}i^2\frac{dL(\theta)}{d\theta} \quad (11)$$

The motor speed can be expressed in terms of the vehicle speed as:

$$\omega_m = m\frac{V_{veh}}{r_{wh}} \quad (12)$$

Where m is the gear ratio of the mechanical coupling between the motor and the axle of the vehicle wheels. Assuming lossless transmission, the developed torque at the shaft of the wheel axle can be determined by:

$$T_{d\_wh} = mT_e \quad (13)$$

The corresponding tractive force will thus be:

$$F_{TR} = \frac{T_{d\_wh}}{r_{wh}} \quad (14)$$

The tractive force developed at the shaft of the wheel axle during acceleration can be expressed by:

$$F_{TR} = k_m M_{veh}\frac{dV_{veh}}{dt} + F_{RL} \quad (15)$$

Where the road load force is (Ehsani *et al*., 1997; Sadeghi *et al*., 2007):

$$F_{RL} = C_0 M_{veh} g + M_{veh} g\sin(\beta) + 0.5\rho C_D A_f V_{veh}^2 \quad (16)$$

Thus, the load torque at the shaft of the wheel axle can be expressed by:

$$T_{wh} = F_{RL}r_{wh} + T_b \quad (17)$$

Also, the load torque at the shaft of the motor axle can be expressed by:

$$T_L = \frac{T_{wh}}{m} \quad (18)$$

Therefore from Eq. 15, the acceleration of the vehicle can be expressed by (Husain and Islam, 1999):

$$\frac{dV_{veh}}{dt} = \frac{1}{k_m M_{veh}}(F_{TR} - F_{RL}) \quad (19)$$

Also using the motor torque and speed, the motor output power can be expressed by:

$$P_{mo} = T_e\omega_m \quad (20)$$

The motor power losses can be determined by:

$$P_{Loss} = n_{ph}I_{ph}^2 R \quad (21)$$

Where I_{ph} is the average value of the motor phase current. The motor excessive energy can be determined from:

$$E_{exc} = n_{ph}\left(I_{ph} - I_r\right)^2 R\,dt \quad (22)$$

Where I_r, dt are the rated value of the motor phase current and the time step.

Algorithm for obtaining results: Starting from zero vehicle speed at constant terminal voltage and certain turn on and turn off angle from Eq. 12, the motor speed would be equal to zero. From Eq. 9 and 10, the motor phase current can be determined. Then using the phase current into Eq. 11, the motor developed Torque (T_e) can be obtained. Also using Eq. 13, the developed torque at the shaft of the wheel axle (T_{d_wh}) can be obtained. The corresponding tractive force (F_{TR}) can thus be obtained from Eq. 14. From Eq. 16, the road load force can be determined at this vehicle speed.

Using these values of the tractive and road load force into Eq. 19, the next vehicle speed can be obtained by integrating this equation numerically over an appropriate time step. For the second and following time steps of numerical solution, the corresponding motor speed is obtained from Eq. 12. Then Eq. 11 is used to obtain its motor developed torque and the corresponding tractive force is obtained from Eq. 14. This process continues until the vehicle reaches steady-state speed.

RESULTS AND DISCUSSION

Performance characteristics of the EV with a variable turn on angle: The approach shown in Fig. 3 was applied using 4th order Runge-Kutta numerical method of integration. Several performance characteristics of the vehicle during acceleration at variable turn on angle and fixed terminal voltage and turn off angle using the data of the SRM and vehicle given in the Appendix are obtained:

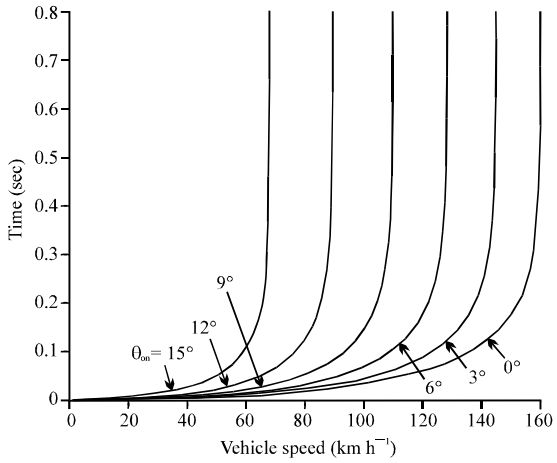

Fig. 3: Vehicle speed vs. time during acceleration with a variable turn on angle

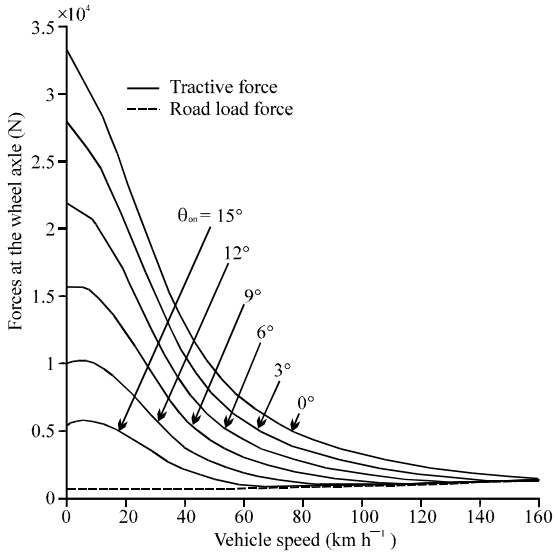

Fig. 4: Tractive and resisting forces at wheel axle vs. vehicle speed during acceleration with a variable turn on angle

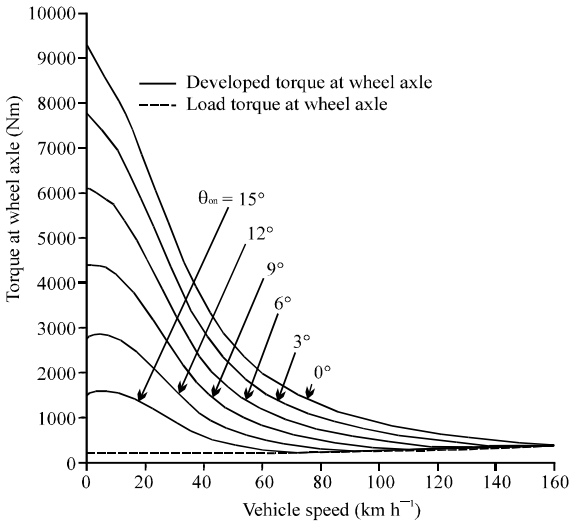

Fig. 5: Torque at wheel axle vs. vehicle speed during acceleration with a variable turn on angle

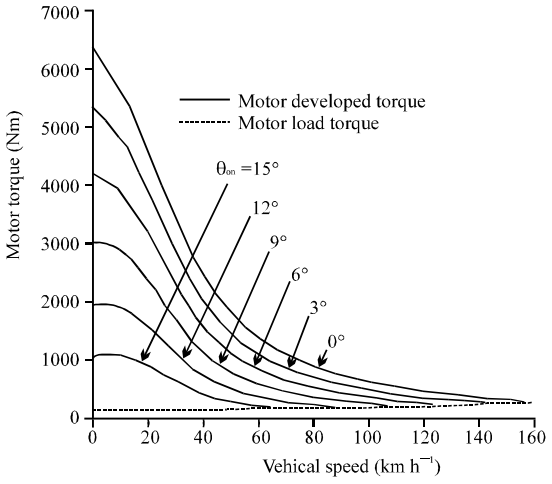

Fig. 6: The motor torque vs. vehicle speed during acceleration with a variable turn on angle

By varying the turn on angle at constant terminal voltage and turn off angle (280 v and 30°, respectively) Figure 3 shows the variation of the vehicle speed throughout the acceleration period. From Fig. 3, it is clear that the vehicle reaches a higher final steady-state speed as the turn on angle decreases.

From Eq. 14 and 16, the tractive and resisting forces (F_{TR}) and (F_{RL}), respectively are plotted against the vehicle speed during the acceleration period until steady-state conditions are reached at the same values of the turn on angle which are used to obtain Fig. 3 as shown in Fig. 4. From Fig. 4, it is clear that for certain turn on angle values, the tractive force decreases and the resisting force increases as the vehicle speed increases up to steady state speed at which the curves of the tractive and resisting forces are intersected. For a certain vehicle speed, the tractive force decreases while the resisting force is constant for the several values of the turn on angle used when their values increase.

From Eq. 13 and 17, the characteristics of the developed and load torque at the shaft of the wheel axle, T_{d_wh} and T_{wh} are obtained against the vehicle speed at different values of the turn on angle as shown in Fig. 5. From Fig. 5, it is noticed that the developed and load torque applied on the wheel axle have the same shape as that of the corresponding tractive and resisting forces shown in Fig. 4 and for the same vehicle

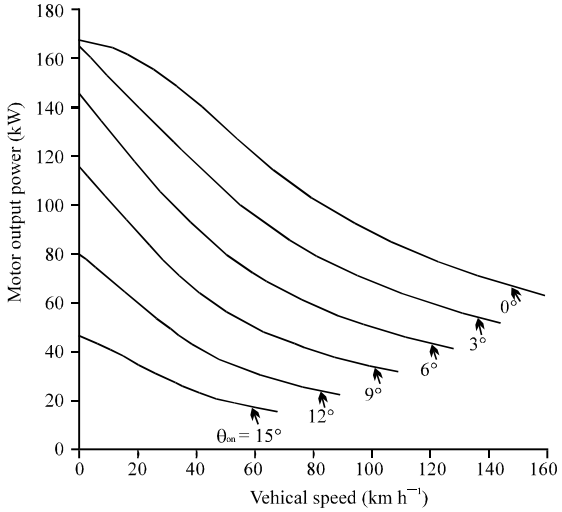

Fig. 7: Motor output power vs. vehicle speed during acceleration with a variable turn on angle

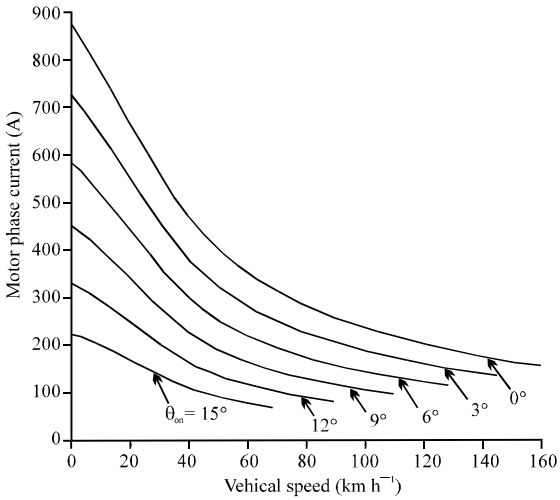

Fig. 8: Motor phase current vs. vehicle speed during acceleration with a variable turn on angle

speed the developed torque decreases as the used values of the turn on angle increase. Using the values of the vehicle speed which are obtained at different values of motor turn on angle into Eq. 9 and 10 then substituting into Eq. 11, the characteristics of the motor developed torque (T_e) can be obtained. Also from Eq. 18, the motor load torque (T_L) can be determined. Then, the motor developed torque and load torque are drawn versus the vehicle speed during acceleration until steady-state conditions are reached as shown in Fig. 6. From Fig. 6, it is clear that for certain turn on angle values, the motor developed torque decreases and the load torque increases as the vehicle speed increases up to steady-state speed at which the curves of the developed and load torques are intersected. For a certain vehicle speed, the developed torque decreases while the load torque is constant for the several values of turn on angle used when their values increase. Using motor developed torque calculated from Eq. 11 and the motor speed calculated from Eq. 12 into 20, the characteristics of the motor output power (P_{mo}) can be obtained against the vehicle speed at different values of the motor turn on angle as shown in Fig. 7. From Fig. 7 for certain values of motor turn on angle, the motor output power decreases as the vehicle speed increases. Also, at certain vehicle speed the developed power has higher values at lower turn on angles.

Using the values of the vehicle speed which are obtained into Eq. 9 and 10, the motor phase current can be determined and plotted against vehicle speed for different values of the motor turn on angle as shown in Fig. 8. From Fig. 8, it is clear that the motor phase current decrease as the vehicle speed increases and for the same vehicle speed, the current decreases as the used values of turn

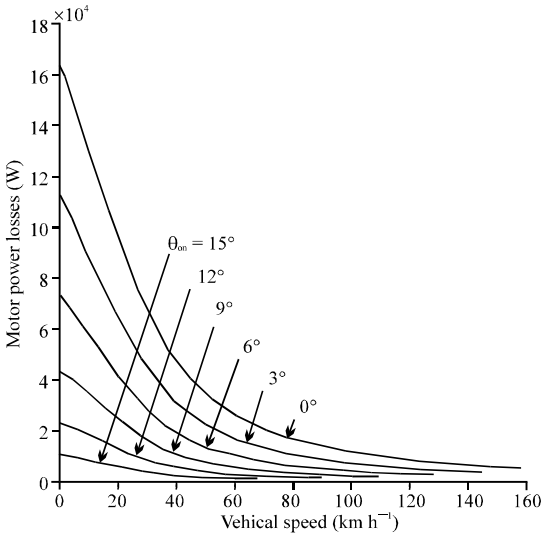

Fig. 9: Motor power losses vs. vehicle speed during acceleration with a variable turn on angle

on angle increase. Using the values of the motor phase current which are obtained at different values of motor voltage into Eq. 21, the characteristics of the motor power losses (P_{Loss}) can be drawn versus the vehicle speed during acceleration until steady-state conditions are reached, as shown in Fig. 9. From Fig. 9, it is noticed that the motor power losses decrease as the vehicle speed increases and for the same vehicle speed the motor losses decreases as the used values of the turn on angle increase. Using the predetermined motor phase current at different values of the motor turn on angle into Eq. 22, the motor excessive energy (E_{exc}) can be computed and plotted as shown in Fig. 10.

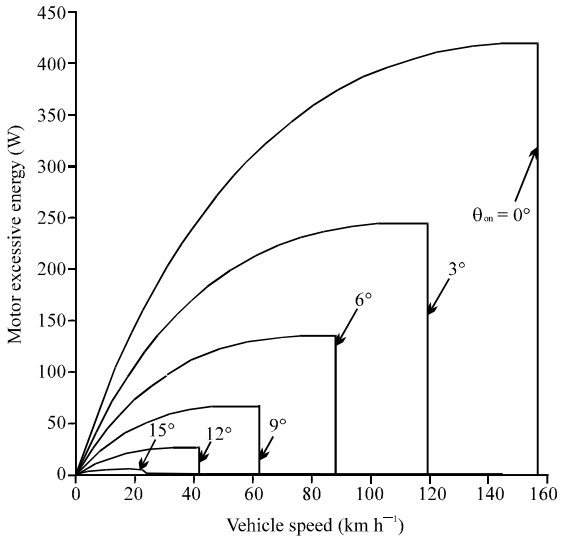

Fig. 10: Motor excessive energy vs. vehicle speed during acceleration with a variable turn on angle

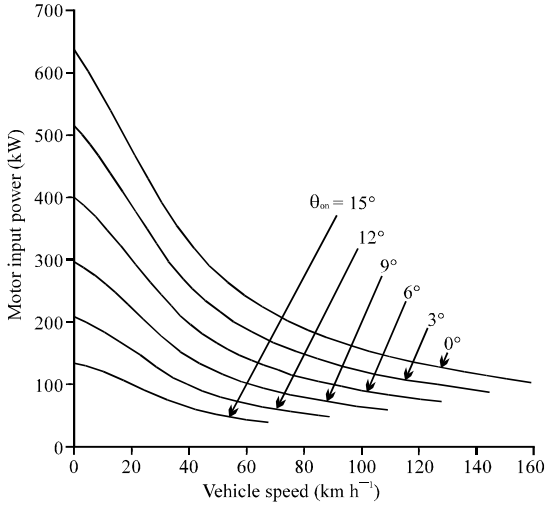

Fig. 11: Motor input power vs. vehicle speed during acceleration with a variable turn on angle

From Fig. 10, it is clear that at certain values of turn on angle, the motor excessive energy increases as the vehicle accelerates then decreases to zero before reaching the final steady state speed. For any vehicle speed, the motor excessive energy will have larger values for lower values of the turn on angle.

Multiplying the predetermined motor phase current which is obtained at different values of the motor turn on angle from Eq. 9 and 10 by the motor terminal voltage, the motor input power (P_{m_in}) can also be computed and plotted as shown in Fig. 11. From Fig. 11, it is clear that at certain values of turn on angle, the motor input power decreases as the vehicle accelerates and reaches

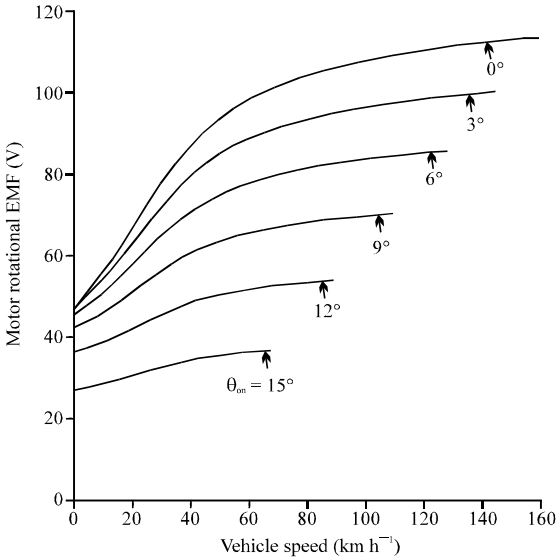

Fig. 12: Motor rotational EMF vs. vehicle speed during acceleration with a variable turn on angle

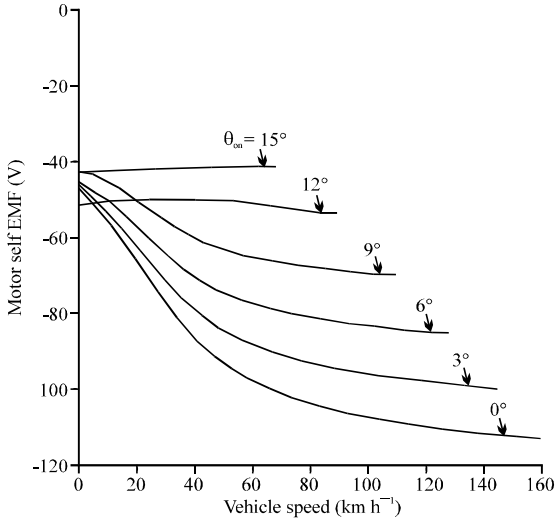

Fig. 13: Motor self EMF vs. vehicle speed during acceleration with a variable turn on angle

a constant value at steady state. For any vehicle speed, the motor input power will have larger values for lower values of the turn on angle.

At certain values of the motor turn on angle from Eq. 6, the motor rotational and self EMF can be calculated, respectively at different values of the vehicle speed. Then, the rotational and self EMF are plotted versus vehicle speed as shown in Fig. 12 and 13, respectively. From Fig.12, it is clear that at a constant turn on angle, the motor rotational EMF increase as the vehicle accelerates and then at a constant vehicle speed the rotational EMF decreases as the turn on angle increase.

From Fig. 13, it is clear that at a constant turn on angle, the motor self EMF decrease as the vehicle accelerates and the rate of decrement increases at lower values of turn on angle. Then at a constant vehicle speed, the self EMF will have larger values for higher values of the turn on angle.

Performance characteristics of the EV with a variable turn off angle: Using the data of the switched reluctance motor and vehicle given in the Appendix, the approach presented in Eq. 3 is repeated using 4th order Runge-Kutta Numerical Method of integration to obtain the performance characteristics of the vehicle during acceleration at variable turn off angle and constant turn on angle and terminal voltage.

By varying the turn off angle at constant turn on and terminal voltage (0° and 280 v, respectively), Fig. 14 shows the variation of the vehicle speed throughout the acceleration period. From Fig. 14, it is clear that the vehicle reaches a higher final steady-state speed as the motor turn off angle increases.

Using Eq. 14 and 16, the tractive and resisting forces F_{TR} and F_{RL}, respectively are plotted against the vehicle speed during the acceleration period until steady-state conditions are reached at the same values of the turn off angle used to obtain Fig. 14 as shown in Fig. 15. From Fig. 15, it is clear that for certain values of the turn off angle, the tractive force decreases and the resisting force increases as the vehicle speed increases up to steady-state speed at which the curves of the tractive and resisting forces are intersected. For a certain vehicle speed, the tractive force decreases while the resisting force is constant for the several values of turn off angle used when their values decrease. From Eq. 13 and 17, the characteristics of the developed and load torque at the shaft of the wheel axle, T_{d_wh} and T_{wh} are obtained against the vehicle speed at different values of the motor turn off angle as shown in Fig. 16. From Fig. 16, it is noticed that the developed and load torque applied on the wheel axle have the same shape as that of the corresponding tractive and resisting forces shown in Fig. 15 and for the same vehicle speed the developed torque decreases as the used values of the turn off angle decrease.

Using the values of the vehicle speed which are obtained at different values of the motor turn off angle

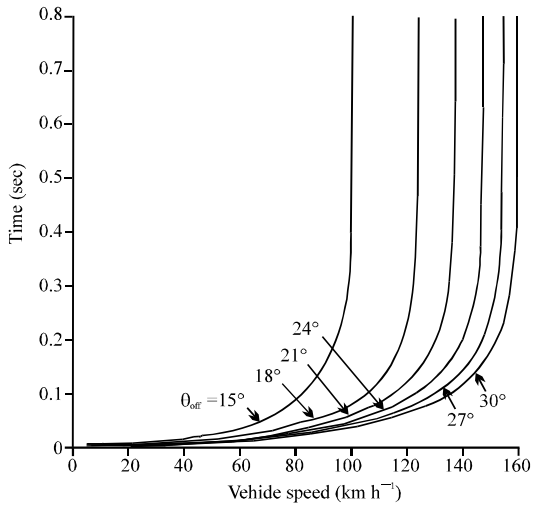

Fig. 14: Vehicle speed vs. time during acceleration with a variable turn off angle

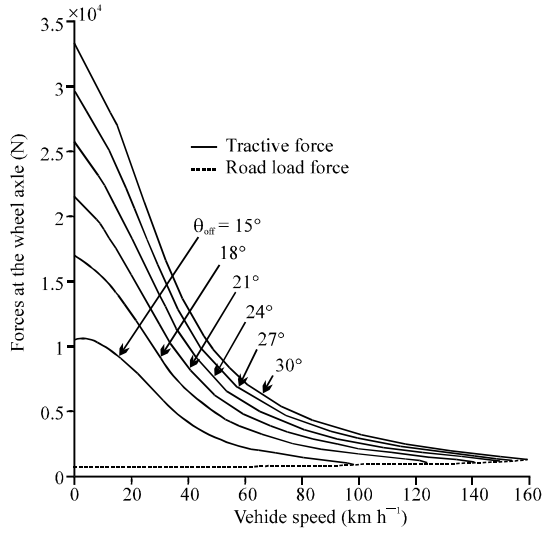

Fig. 15: Tractive and resisting forces at wheel axle vs. vehicle speed during acceleration with a variable turn off angle

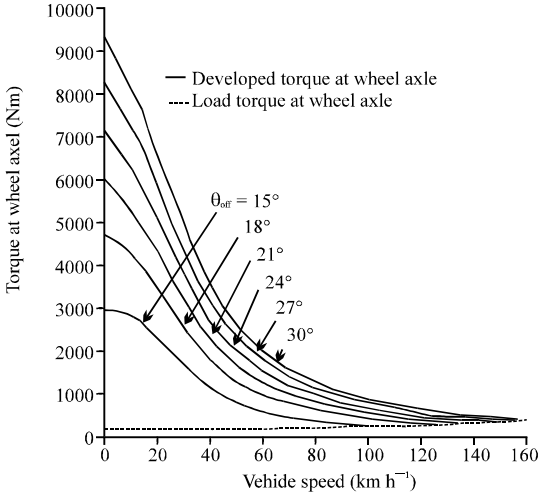

Fig. 16: Torque at wheel axle vs. vehicle speed during acceleration with a variable turn off angle

into Eq. 9 and 10 then substituting into Eq. 11, the characteristics of the motor developed torque (T_e) can be obtained. Also from Eq. 18, the motor load torque (T_L) can be determined.

Then, the motor developed torque and load torque are drawn versus the vehicle speed during acceleration until steady-state conditions are reached as shown in Fig. 17. From Fig. 17, it is clear that for certain values of the turn off angle, the motor developed torque decreases and the load torque increases as the vehicle speed increases up to steady-state speed at which the curves of the developed and load torques are intersected. For a certain vehicle speed, the developed torque decreases while the load torque is constant for the several values of turn off angle used when their values decrease.

Using the motor developed torque calculated from Eq. 11 and the motor speed calculated from Eq. 12 into 20, the characteristics of the motor output power (P_{mo}) can be obtained against the vehicle speed at different values of the motor turn off angle as shown in Fig. 18.

From Fig. 18 for certain values of motor turn off angle, the motor output power decreases as the vehicle speed increases. Also at certain vehicle speed the developed power has higher values at higher turn off angle.

Using the values of the vehicle speed which are obtained into Eq. 9 and 10, the motor phase current can be determined and plotted against vehicle speed for different values of the motor turn off angle as shown in Fig. 19. From Fig. 19, it is clear that the motor phase current decrease as the vehicle speed increases and for the same vehicle speed the current decreases as the used values of the turn off angle decrease.

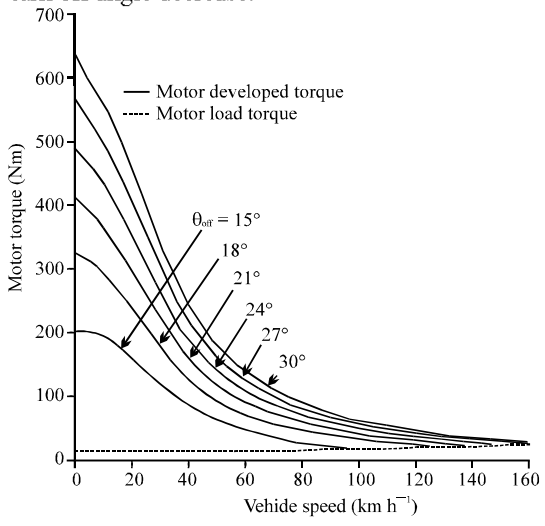

Fig. 17: The motor torque vs. vehicle speed during acceleration with a variable turn off angle

Using the values of the motor phase current which are obtained at different values of motor turn off angle into Eq. 21, the characteristics of the motor power losses (P_{Loss}) can be drawn versus the vehicle speed, during acceleration until steady-state conditions are reached as shown in Fig. 20.

From Fig. 20, it is noticed that the motor power losses decrease as the vehicle speed increases and for the same vehicle speed the motor losses decreases as the values of the turn off angle decrease. Using the predetermined motor phase current at different values of the motor turn off angle into Eq. 22, the motor excessive energy (E_{exc})

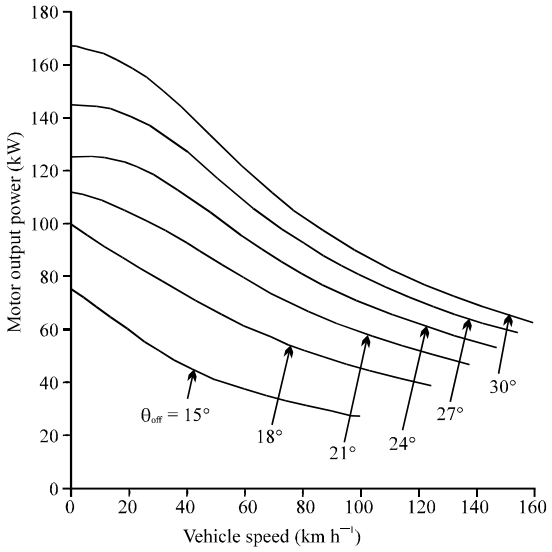

Fig. 18: Motor output power vs. vehicle speed during acceleration with a variable turn off angle

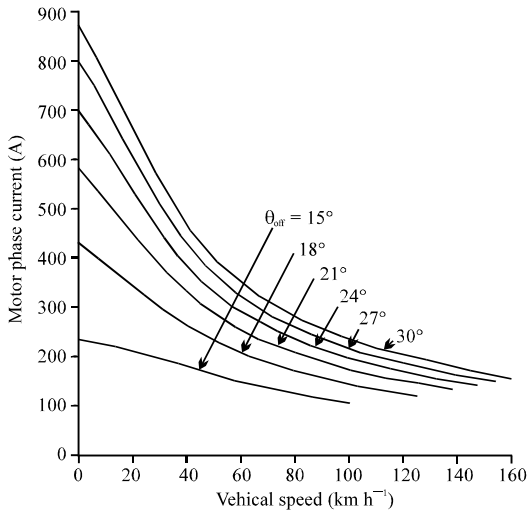

Fig. 19: Motor phase current versus vehicle speed during acceleration with a variable turn off angle

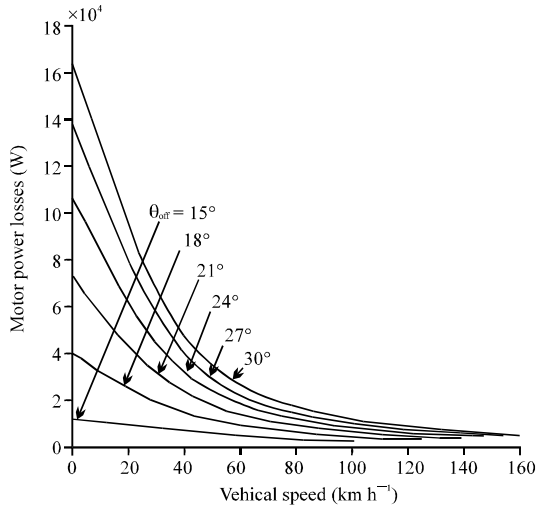

Fig. 20: Motor power losses vs. vehicle speed during acceleration with a variable turn off angle

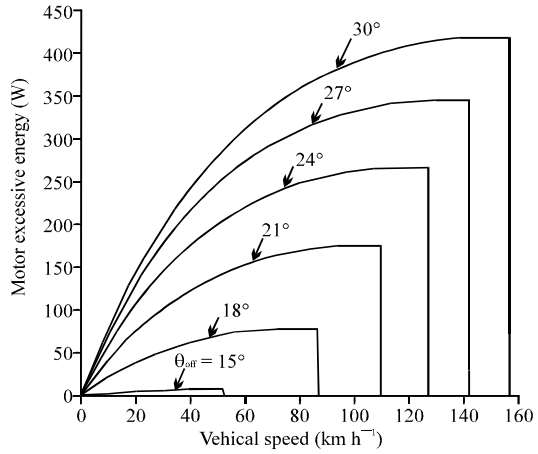

Fig. 21: Motor excessive energy vs. vehicle speed during acceleration with a variable turn off angle

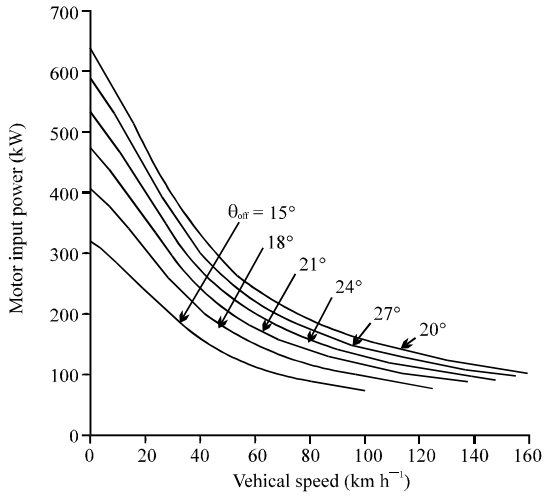

Fig. 22: Motor input power vs. vehicle speed during acceleration with a variable turn off angle

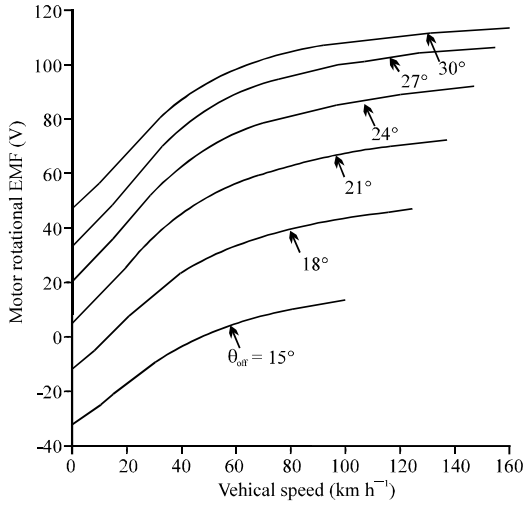

Fig. 23: Motor rotational EMF vs. vehicle speed during acceleration with a variable turn off angle

can be computed and plotted as shown in Fig. 21. From Fig. 21, it is clear that at certain values of the turn off angle, the motor excessive energy increases as the vehicle accelerates then decreases to zero before reaching the final steady state speed. For any vehicle speed, the motor excessive energy will have larger values for higher values of the turn off angle.

Multiplying the predetermined motor phase current which is obtained at different values of the motor turn off angle from Eq. 9 and 10 by the motor terminal voltage, the motor input power (P_{m_in}) can be also computed and plotted as shown in Fig. 22. From Fig. 22, it is clear that at certain values of the turn off angle, the motor input power decreases as the vehicle accelerates and reaches a constant value at steady state. For any vehicle speed, the motor input power will have larger values for higher values of the turn off angle.

At certain values of the motor turn off angle from Eq. 6, the motor rotational and self EMF can be calculated, respectively at different values of the vehicle speed. Then, the rotational and self EMF are plotted versus vehicle speed as shown in Fig. 23 and 24, respectively.

From Fig. 23, it is clear that at a constant turn off angle, the motor rotational EMF increase as the vehicle accelerates and then at a constant vehicle speed the rotational EMF decreases as the turn off angle decreases.

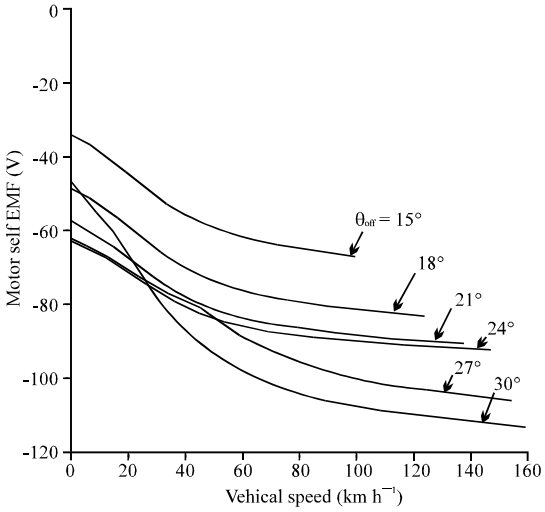

Fig. 24: Motor self EMF vs. vehicle speed during acceleration with a variable turn off angle

From Fig. 24, it is clear that at a constant turn off angle, the motor self EMF decrease as the vehicle accelerates and the rate of decrement increases at higher values of turn off angle. Then at a constant vehicle speed, the self EMF will have larger values for lower values of the turn off angle.

CONCLUSION

From the performance characteristics of the EV operating in the acceleration mode, the following is observed as the motor turn on decreases and turn off angle increases:

- The vehicle reaches a higher final steady-state speed
- The tractive force increases while the resisting force is constant for a certain vehicle speed
- The motor developed torque increases for a certain vehicle speed while the load torque is constant
- The motor developed power has higher values at certain vehicle speed
- The motor phase current will have larger values for any vehicle speed
- The motor power losses has higher values at certain vehicle speed
- The motor excessive energy has larger values at certain vehicle speed
- The motor input power increases at a constant vehicle speed
- The motor rotational EMF has larger values at a constant vehicle speed
- The motor self EMF has lower values at a constant vehicle speed

Also for certain operating values of the motor turn on and turn off angle:

- The tractive force decreases and the resisting force increases as the vehicle speed increases up to steady-state speed at which the tractive and resisting forces are equal
- The motor developed torque decreases and the load torque increases as the vehicle speed increases up to steady-state speed
- The motor developed power decreases as the time increases until the vehicle reaches steady-state speed at which the developed power becomes constant
- The motor phase current decreases as the vehicle accelerates and reaches a constant value at steady state
- The motor power losses decreases as the vehicle accelerates
- The motor excessive energy increases as the vehicle accelerates then decrease to zero value near the final steady-state speed
- The motor input power decreases as the vehicle accelerates
- The motor rotational EMF increases as the vehicle speed increases up to steady-state speed
- The motor self EMF decreases as the vehicle accelerates

NOMENCLATURE

A_f = Equivalent frontal area of the vehicle in m^2
C_0 = Coefficient of rolling resistance
C_D = Aerodynamic drag coefficient
E_{exc} = Motor excessive energy
F_{RL} = Road load force in N
F_{TR} = Tractive force in N
g = Gravitational acceleration constant in m sec^{-2}
i = Motor phase current
I_{ph} = The average value of the motor phase current in A
I_r = Rated value of the motor phase current in A
k_1-k_4 = Constants
k_m = Rotational inertia coefficient
L = Motor phase inductance
L_a = Aligned inductance in mH
L_u = Unaligned inductance in mH
m = The gear ratio of the mechanical coupling between the motor and the axle of the vehicle wheels
M_{veh} = Total mass of the vehicle in kg
n_{ph} = Number of motor phases

N_r = Number of rotor poles
P_{Loss} = Motor power losses in W
$P_{m\text{-}in}$ = Motor input power in W
P_{mo} = Motor output power in W
R = Motor phase resistance in ohm
r_{wh} = Radius of the wheel in m
T_b = Frictional brake torque in Nm
T_{d_wh} = The developed torque at the shaft of the wheel axle
T_e = Motor developed torque in Nm
T_L = Load torque at the shaft of the motor axle in Nm
T_{wh} = Load torque at the shaft of the wheel axle in Nm
ν = Motor phase voltage in v
V_s = DC supply voltage in v
V_{veh} = Vehicle speed in km h^{-1}
β = Road grade angle
β_r = Rotor poles arc
θ = Rotor position in elec.rad
θ_0 = The angle at which the motor phase current equal zero after decaying
θ_{off} = Turn off angle
θ_{on} = Turn on angle
λ = Motor phase flux linkage
ρ = Air density in kg m^{-3}
ω = Motor speed in elec.rad sec^{-1}
ω_m = Motor speed in rad sec^{-1}

APPENDIX

Data of the SRM: P_r = 60 kW, V_r = 280 V, R = 0.072 Ω, L_a = 3.334 mH, L_u = 0.445 mH, Nr = 4, Ns = 6, n_{ph} = 3, Bs = Br = π/6, j = 0.3, b = 0.0183,n_r = 2214 rpm.

Vehicle dynamic parameters: ρ = 1.225 kg m^{-3}, C_D = 0.3, A_f = 2 m^2, M_{veh} = 1500 kg, r_{wh} = 0.2794 m, Tb = 0, $V_{veh\text{-}max}$ = 160 km h^{-1}, V_f = 100 km h^{-1}, km = 1.08, C_0 = 0.01, g = 9.81 m sec^{-2}, m = 1.4575, β = 2°, η_{tmw} = 0.95.

REFERENCES

Ehsani, M., K.M. Rahman and H.A. Toliyat, 1997. Propulsion system design of electric and hybrid vehicles. IEEE Transact. Indus. Electron., 44: 19-27.

Ehsani, M., Y. Gao, S.E. Gay and A. Emadi, 2005. Modern Electric, Hybrid Electric and Fuel Cell Vehicles: Fundamentals, Theory and Design. CYC Press, Boca Raton, Fla.

Husain, I. and M. Islam, 1999. Design, modeling and simulation of an electric vehicle system. SAE Technical Paper 1999-01-1149, Society of Automotive Engineers (SAE). http://papers.sae.org/1999-01-1149/.

Husain, I., 2005. Electric and Hybrid Vehicles Design Fundamentals. Taylor and Francis, New York.

Rahman, K.M., B. Fahimi, G. Suresh, A.V. Rajarathnam and M. Ehsani, 2000. Advantages of switched reluctance motor applications to EV and HEV: Design and control issues. IEEE Trans. Industry Applic., 36: 111-121.

Sadeghi, S., J. Milimonfared and M. Mirsalim, 2007. Dynamic modeling and simulation of a series hybrid electric vehicle using a switched reluctance motor. Proceedings of the International Conference on Electrical Machines and Systems, Octuber 8-11, 2007, Seoul, pp: 2017-2022.